Scaled-Up Slack Generator Based on Parallel Inverters for a Reliable IFSA Microgrid

SOO HYOUNG LEE, (Member, IEEE)

Department of Electrical and Control Engineering, Mokpo National University, Jeollanam-do 58554, South Korea

e-mail: slee82@mokpo.ac.kr

ABSTRACT It is expected that the penetration of renewable-energy-based generators will rapidly increase worldwide. These factors also lead to an increase in the portion of inverters in the power system. This paper proposes a method to scale up the slack generator size based on parallel inverters. All of the multiple parallel inverters except one share the measured power from the slack bus to the grid by a predetermined ratio based on their sizes. A single inverter that does not participate in power sharing is allocated to be in charge of clearing the small power gap caused by the control delay and the measurement error (i.e., the physical slack). As a result, the net size of the scaled-up slack generator is n times greater than that of the physical slack when n non-slack inverters are added to the physical slack inverter. The proposed method is validated based on a real island power system model in Korea using a power system computer-aided design/electromagnetic transient including DC (PSCAD/EMTDC^{TM}).

INDEX TERMS DG acceptability, large IFSA microgrid, load sharing, parallel inverter connection, scale-up of slack generator.

I. INTRODUCTION

A. MOTIVATION AND INCITEMENT

Since the recent advent of COVID-19, ESG (environmental, social, governance) considerations have emerged as very important factors even for businesses. Especially in regard to environmental issues, CO_2 emissions must be reduced to below 45% of the 2010 levels by 2030 to limit the global warming to under 1.5°C [1]. Relatedly, the Korean government plans to implement "renewable energy 3020", which aims to increase the country's dependency on renewable energy sources by up to 20% by 2030 [2]. In particular, more than 80% of the power generated from renewable energy sources will be variable renewable energy (VRE), which is fluctuating in nature, such as solar and wind.

Despite the positive aspects of global movements, there are many technical issues to be discussed. One of them is the power system voltage stability. Even though the Korean power system currently has very good stability, it becomes difficult to keep it in good condition with increasing

renewable energy sources, which are connected to the system via power inverters [3], [4].

The voltage of a conventional generator bus in a power system is kept constant with the control of the excitation system, but it is difficult to apply the same approach for DGs with VRE connected through a converter. In addition, the real and reactive power control of the converter might impact the bus voltage, which must be used as a reference point for power control because of the converter's controlling nature.

B. LITERATURE REVIEW

To improve the voltage stability in an inverter-based system, synchronized GPS-time-based multiple slack bus control is proposed [5]. The key prerequisite, however, for multiple slack bus control is the inverter size. The inverter cannot operate as the slack generator for power system events exceeding the inverter size. In practice, nevertheless, the inverter size is much smaller than that of a conventional generator. Therefore, a group composed of multiple inverters is required for slack operation. Only one inverter can be in charge of common bus voltage control to avoid hunting between multiple voltage controls on the same bus. Therefore, the net size of the

slack generator is the same as that of the voltage-controlled inverter even if there are numerous inverters. As a result, power sharing among multiple inverters is the key technology to enlarge the effective size of the inverter-based slack generator.

Sliding mode control is studied to support the grid voltage by grid-connected inverters even in weak grid conditions such as distorted grid voltage [6]. Although this method is useful when the voltage given by the grid is weak, the inverter cannot operate as a reference of the entire grid voltage. Sensorless model predictive control is studied under unbalanced and distorted grid voltages [7]. This method requires very accurate grid impedance information for the prediction. In practice, however, the equivalent grid impedance is not known and even changes over time.

Many researchers have applied droop-based control to multiple inverters in power systems for power-sharing. A virtual impedance-based droop control was proposed to improve the flexibility of P-f and Q-V control [8]. Droop control in the d-q axis has also been proposed [9]. There is also a droop control approach to limit the current [10]. The main purpose of this control is to protect the device from unrealistically large currents. In addition, there have been stability studies for not only determining the stable region by adjusting the droop ratio of conventional P-f and Q-V droop controls [11], [12] but also for calculating the damping ratio automatically to reduce the oscillations [13]. However, the proposed methods might not be feasible to implement in a single bus.

A droop-free distributed control method [14], a stochastic control method [15], and power flow analysis-based approaches [16], [17] have been developed to overcome the limitations of conventional droop-based control in a multibus power system. In a single bus, however, the drawbacks of the droop-free method become rather pronounced due to the high dependency on communication and mathematical uncertainty.

There are also several studies of virtual synchronous generators [18]–[21]. These methods limit the responses of the converters to the synchronous generator and thus, make it rather worse because the multiple inverters play the role of a virtual large single inverter.

Robust repetitive control of the inverter is studied for stand-alone operation [22]. This method, however, considers only a single inverter operation rather than that of multiple inverters. In addition, this method does not avoid the problem of control hunting between multiple inverters. There is also a study of voltage control based on the expanded inverse model of the inverter [23]. This method, however, does not require multiple inverter operations on the same bus. Additionally, it requires substantial computational effort for neural network applications. Virtual multi-slack (VMS) control [24], [25] is useful to control bus voltages without hunting between multiple inverters. However, it is not feasible for multiple inverters in a single bus because the admittance matrix becomes infinite.

C. CONTRIBUTION AND PAPER ORGANIZATION

In this paper, a scaled-up slack generator is virtually implemented by multiple inverters connected to a single common bus. The required power is shared among the inverters based on aggregated power measurement from the common bus to the grid. A single inverter is allocated to be in charge of clearing the small power gap caused by the control delay and the measurement error.

The multiple inverter-based scaled-up slack generator allows a large size inertia-free stand-alone (IFSA) microgrid [5] even if the size of each inverter is small. It overcomes the shortages of the conventional power-sharing methods such as droop and VMS etc., by the parallel connection of multiple inverters on a single bus. Also, the scaled-up slack generator can be simply applied to solid-state transformers [26], [27]. The small current rating of the power electronics switch can be overcome by the parallel-connected multiple solid-state transformers. This results in a simple expansion of the capacity of the solid-state transformer by means of a multi-level topology together.

This paper is organized as follows. First, the problem formulation is described in Section II. Then, a scaled-up slack generator is proposed in Section III. Thereafter, the changeover between the slack and PQ modes is given in Section IV. After that, case studies are shown in Sections V-VIII. Finally, the conclusion is given in Section IX.

II. PROBLEM FORMULATION

IFSA microgrid has no synchronous generators and is powered only from inverters so that it does not have physical rotational inertia [5]. At least one inverter must be operated in slack control to prevent severe frequency variation caused by zero rotational inertia. To apply the GPS time synchronization based IFSA microgrid operation method to a large IFSA microgrid, some of the DGs might need to be scaled up for proper power supply. As is commonly known, the size of the DG can be scaled up by increasing the voltage or current ratios. To use high voltage, the DG might require MMC because of the limitation of the maximum voltage rating of commercial IGBTs. However, MMCs are much more complicated than single-level inverters, so they might be exposed to malfunctions more frequently than single-level inverters. In contrast, the size of the DG can be scaled up easily using a large current by parallel connection of multiple single-level inverters. In this case, malfunctions of some inverters could not be a serious problem owing to the normal operation of the other inverters. The situation can be simply resolved by removing the faulty inverters.

Every DG in the IFSA microgrid directly controls the magnitude and phase angle of its connected bus voltage. The real and reactive powers from the DG are calculated as

$$P_i = \sum_{j=1}^{n} |V_i||V_j||Y_{ij}|\cos(\theta_{ij} - \delta_i + \delta_j) \qquad (1)$$

$$Q_i = -\sum_{j=1}^{n} |V_i||V_j||Y_{ij}|\sin(\theta_{ij} - \delta_i + \delta_j) \qquad (2)$$

where i and j are the DG connected and adjacent buses, respectively. V_i and δ_i are the voltage and phase angle on bus i, respectively. Y_{ij} and θ_{ij} are magnitude and phase angle components, respectively, of the admittance matrix related to buses i and j. In general, small control errors of the DGs are not a problem. This is because errors between multiple DGs do not have a significant impact on the power flows due to impedance. In the case of multiple inverters connected on the same bus, by contrast, large power flows can damage the inverters because of the extremely small impedance (i.e., extremely large $|Y|$) of the bus bar. Therefore, only one inverter must be given the right to control the magnitude and phase angle of the bus voltage (i.e., the slack DG).

III. SCALED-UP SLACK GENERATOR
To scale up the slack DG, multiple inverters are connected to a bus, as shown in Fig. 1, including one slack-controlled inverter.
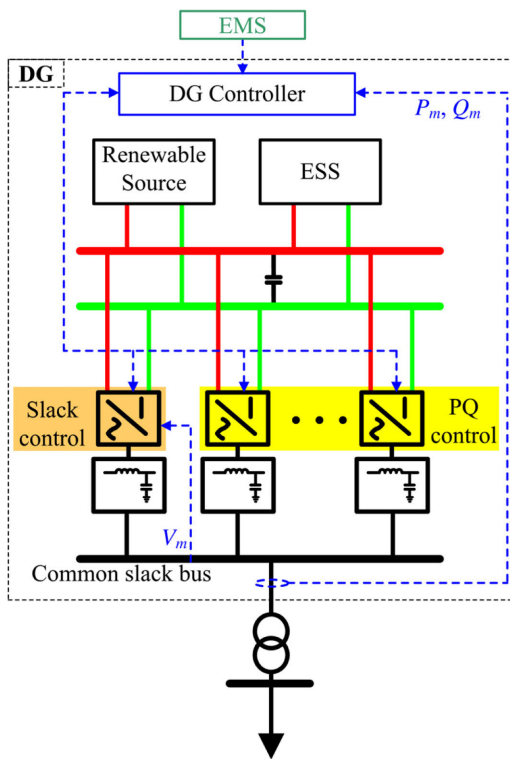

FIGURE 1. Scaled-up slack DG including one slack and multiple real and reactive power-controlled inverters.

In the scaled-up slack DG, the real and reactive power references for the PQ-control mode inverters are determined by

$$P_{n,ref} = x_n P_m \qquad (3)$$
$$Q_{n,ref} = x_n Q_m \qquad (4)$$

where P_m and Q_m are the real and reactive powers, respectively, that flow from the common bus to the transformer. The number of PQ-control mode inverters is denoted by n. The weight x is determined in proportion to the size of the inverter. In other words, the sum of the weights must be one. Moreover, the slack controlled inverter operates based on (5), similar to the other inverter-based slack generators.

$$V_{sa} = V_p \sin(\omega t + \theta)$$
$$V_{sb} = V_p \sin\left(\omega t + \frac{2}{3}\pi + \theta\right)$$
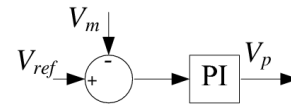$$V_{sc} = V_p \sin\left(\omega t - \frac{2}{3}\pi + \theta\right) \qquad (5)$$

FIGURE 2. Voltage magnitude controller for the slack-controlled inverter of the scaled-up slack DG.

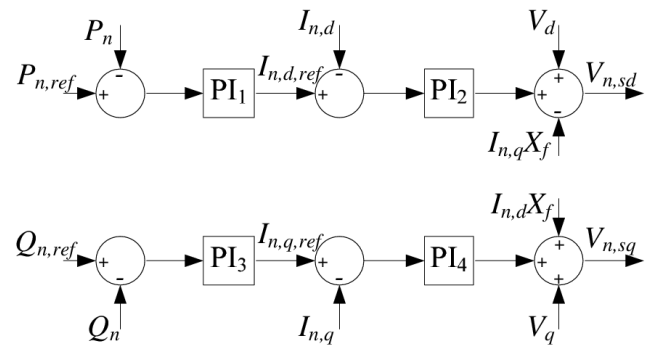**FIGURE 3. Real and reactive power controller for the nth PQ-control mode inverter of the scaled-up slack DG.**

where V_s and V_p are the instant terminal voltage of the inverter and its peak value, respectively. The phase angle of the terminal voltage and the rated system frequency are denoted by θ and ω, respectively. To keep the magnitude of the voltage constant on the common slack bus, V_p is controlled by Fig. 2. where V_m is the measured magnitude of the common slack bus voltage. When V_m is smaller than the reference V_{ref}, V_p increases to raise V_m to V_{ref}. In the opposite case, V_p decreases to reduce V_m to V_{ref}. The slack-controlled inverter uses fixed θ regardless of the grid condition. This is because the PQ-control mode inverters share all of the load by (3)-(4) so that the power from the slack-controlled inverter is zero in the steady state. Therefore, the common slack bus can maintain a constant phase angle of voltage without complicated phase control. Meanwhile, each PQ-control mode inverter operates by well-known real and reactive power controllers, as shown in Fig. 3. The direct and quadrature axis terminal voltage references are transformed into three-phase references by synchronous inverse Park's transformation. As a result, the PQ-control mode inverters are in charge of

load sharing. In contrast, the slack controlled inverter is in charge of maintaining the voltage on the common slack bus and finely balancing the load and generation.

IV. CHANGE-OVER BETWEEN SLACK AND PQ MODES

To improve the reliability of the IFSA microgrid, every inverter in a DG must have the ability to operate in slack control mode. To prepare the sudden trip of the slack-control mode inverter, one of the PQ mode inverters is selected as a back-up slack during its operation as shown in Fig. 4.

First, it is determined whether a PQ-control mode inverter remains. If there is no remaining PQ-control mode inverter, the DG does not select a back-up slack inverter and terminates the selection process. This is because there is no inverter in operation except the slack-control mode inverter. In contrast, the DG selects a back-up slack inverter if there is at least one PQ-control mode inverter. Next, the DG checks if the back-up slack-control mode inverter is on. If the back-up slack-control mode inverter is off, the process returns to check the remaining PQ-control mode inverters. In the case that the back-up slack-control mode inverter is on, the DG checks if the slack-control mode inverter is on. If the slack inverter is on, the process goes back to check the back-up slack-control mode inverter. The back-up slack-control mode inverter changes its operation mode from PQ control to slack immediately if the original slack-control mode inverter is off. The entire process repeats until there is no remaining PQ-control mode inverter. To apply the proposed changeover process to the DG, each inside inverter must be able to operate in the slack-control mode as well as in the PQ-control mode. Additionally, the grid impact must be minimized during the mode transition.
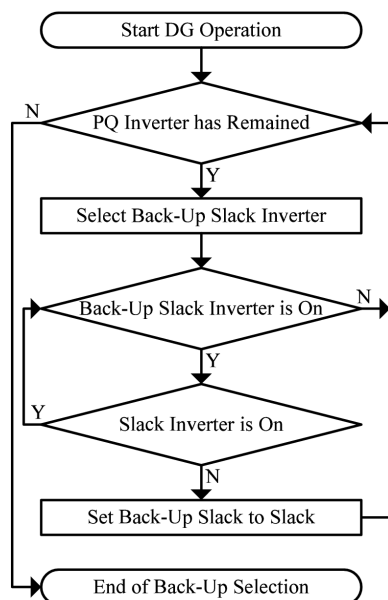

FIGURE 4. Flow diagram of the operation mode change-over in the individual scaled-up slack DG.

To achieve these goals, each inverter controller is implemented, as shown in Fig. 5. In PQ-control mode, the left side

of the 'hold on data in slack mode' block operates in the same manner as the PQ controller in Fig. 3. Meanwhile, the 'hold on data in slack mode' block passes the input data as it is, and the root-mean-square bus voltage (V_{rms}) is not controlled. The 'dq to abc' block operates based on the following equation.

$$
\begin{bmatrix} V_{sa} \\ V_{sb} \\ V_{sc} \end{bmatrix} = \sqrt{\frac{2}{3}} \begin{bmatrix} \cos(\Theta) & \sin(\Theta) \\ \cos(\Theta - \frac{2}{3}\pi) & \sin(\Theta - \frac{2}{3}\pi) \\ \cos(\Theta + \frac{2}{3}\pi) & \sin(\Theta + \frac{2}{3}\pi) \end{bmatrix} \begin{bmatrix} V_{sd} \\ V_{sq} \end{bmatrix}
$$

(6)

where $\Theta = \omega t + \theta$. For the PQ-control mode, the phase angle from the synchronized reference dq-transformation, θ_{synch} is used for θ. The rated system frequency and GPS-based synchronized time in [5] are used for ω and t, respectively. In slack-control mode, by contrast, the PQ controller does not work by making the inputs of PI_1 to PI_4 zero. Additionally, V_{rms} is controlled (instead of the real and reactive powers) by PI_5, and the phase angle of the bus voltage θ_m is controlled by PI_6 to follow θ_{ref}. The result of PI_6, θ determines the phase angle of the terminal voltage. At the moment of the change-over to the slack-control mode, θ is the same as the last value of θ_{synch}, and the captured constant data by 'hold on data in slack mode' blocks are used for the magnitude of voltage control to minimize the transition impact on the grid. In other words, the outputs of the 'hold on data in slack mode' blocks in the slack-control mode are fixed as the last values of the PQ-control mode. Finally, $V_{rms,ref}$ and θ_{ref} are determined by an upper-level microgrid control center described in [5].

V. CASE STUDIES WITH INTERNAL CHANGES

The proposed scaled-up slack generator is verified using a practical stand-alone microgrid as shown in Fig. 6, which is composed of real island power system data in Korea. Here, two scaled-up slack generators are connected to buses 9 and 23. The diesel generators on bus 1 in the original system are substituted by the proposed scaled-up slack generator.

For the verification, the scaled-up DG in bus 9 is manipulated. The output is set as 1 MW and 0.1 MVAr by adjusting the microgrid. The scaled-up DG is initially composed of ten PQ-control mode inverters and one slack control mode inverter. Each PQ-control mode inverter is in charge of 0.1 MW and 0.01 MVAr load. The slack-control mode inverter only complements the difference between the generation and load caused by the delayed response of the PQ-control mode inverters. Its average output is set close to zero. In this case, the DG is exposed to the most severe situation when only the slack control mode inverter is disconnected.

A. SLACK INVERTER DISCONNECTION

The back-up slack generator operates in PQ-control mode when the slack-control mode generator operates normally. The back-up slack generator should take over the initial slack
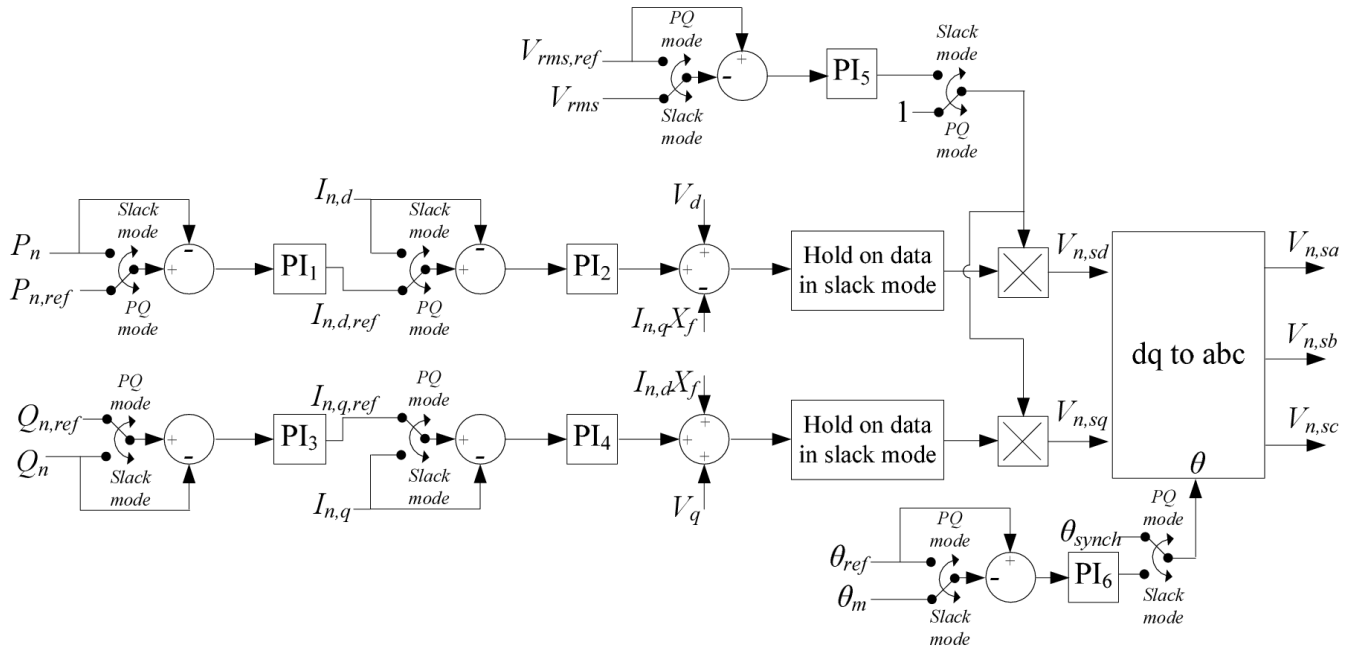
FIGURE 5. Inverter controller including the changeover between slack and PQ control.
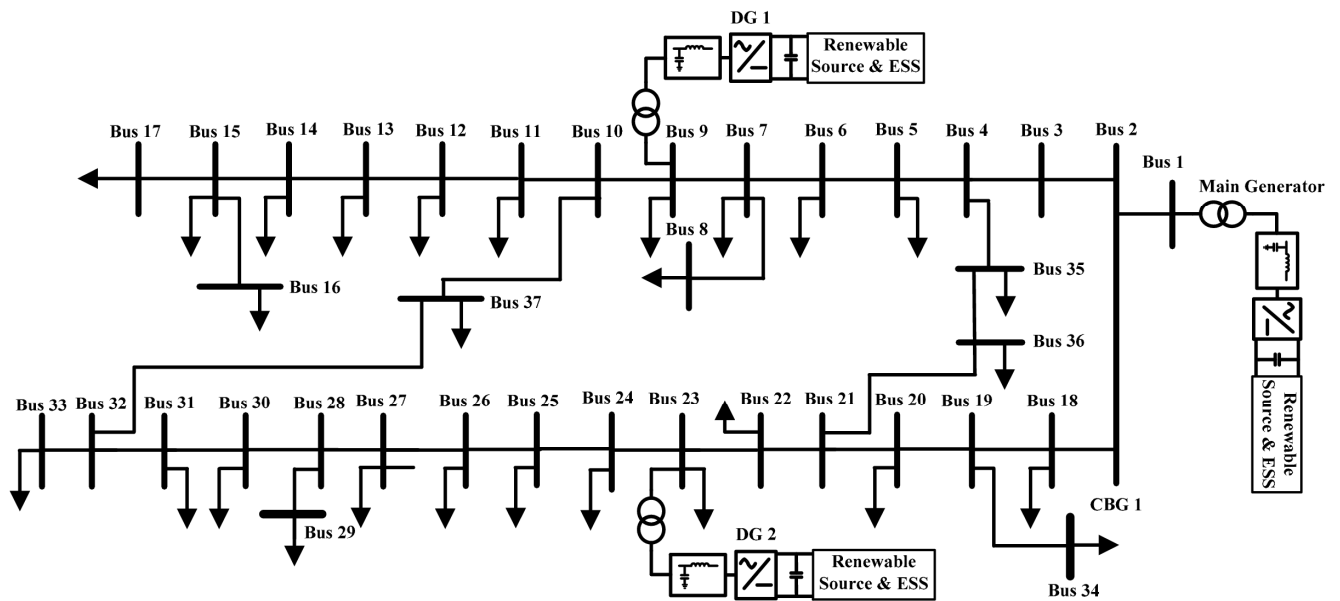

FIGURE 6. Practical stand-alone microgrid model with 37 buses composed of a real island power system data in Korea.

generator's role when the initial slack generator is disconnected, as described in Fig. 4.

As shown in Fig. 7(e), one of the PQ-control mode inverters (i.e., the back-up slack) starts to operate in slack-control mode when the original slack-control mode inverter is disconnected at 0.5 seconds. Initially, the original slack inverter generates near-zero power so that the impact from the disconnection of the inverter is quite limited. Therefore, the grid voltage and phase are maintained during the short time

of the control mode change of the back-up slack inverter from PQ-control to slack-control. After the transition to slack control mode, the DG controller increases the output powers of the remaining PQ-control mode inverters up to approximately 0.111 MW and 0.0111 MVAr to make the average output power of the new slack-control mode inverter be set close to zero (Figs. 7(a)-(b)). The magnitude and phase angle variation of the bus voltage is smaller than 0.01 pu and 0.01 radians during the rebalancing of power

between the remaining PQ-control mode inverters as shown in Figs. 7(c)-(d).
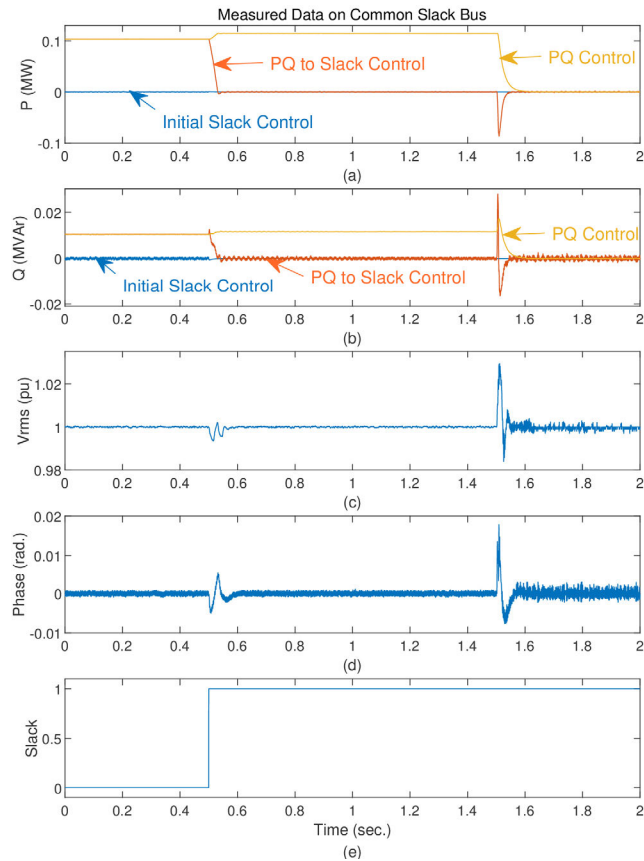
FIGURE 7. Inverter responses to the initial slack control mode inverter disconnection (0.5 seconds) and the entire load disconnection (1.5 seconds): initial slack control mode inverter (blue line), back-up slack inverter (orange line), and a representative of other PQ-control mode inverters (yellow line).

The new slack control mode inverter even effectively responds to the most severe load change (i.e., entire load disconnection at 1.5 seconds), similar to the general slack generator. It consumes at most approximately 0.1 MW and 0.02 MVAr from the PQ-control mode inverters to match the generation to no load (Figs. 7(a)-(b)). The momentary increases in magnitude and phase angle of voltage are caused by the real and reactive power absorption of the slack control mode inverter (Figs. 7(c)-(d)). These values are limited to approximately 0.025 pu and 0.02 radians.

B. ADDITIONAL INVERTER CONNECTION
As described above, the scaled-up slack generator maintains its slack performance if there is at least one normally operating inverter. Therefore, only PQ-control mode inverters can be additionally connected to the same bus to avoid collisions between multiple slacks. As shown in Figs. 8(c)-(d), there are no remarkable variations in the magnitude and phase angle of the bus voltage. After the connection of the additional inverter, the DG controller gradationally increases the output
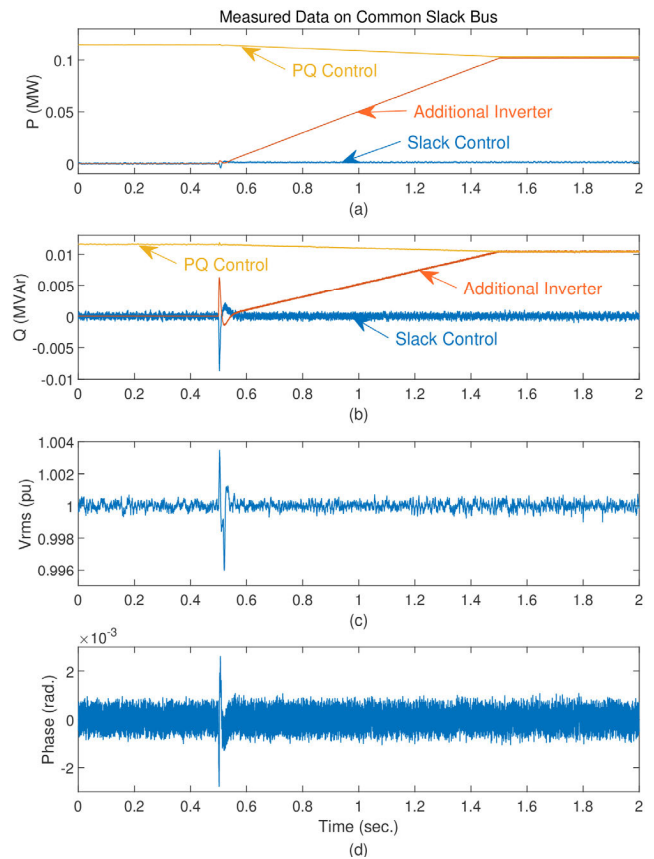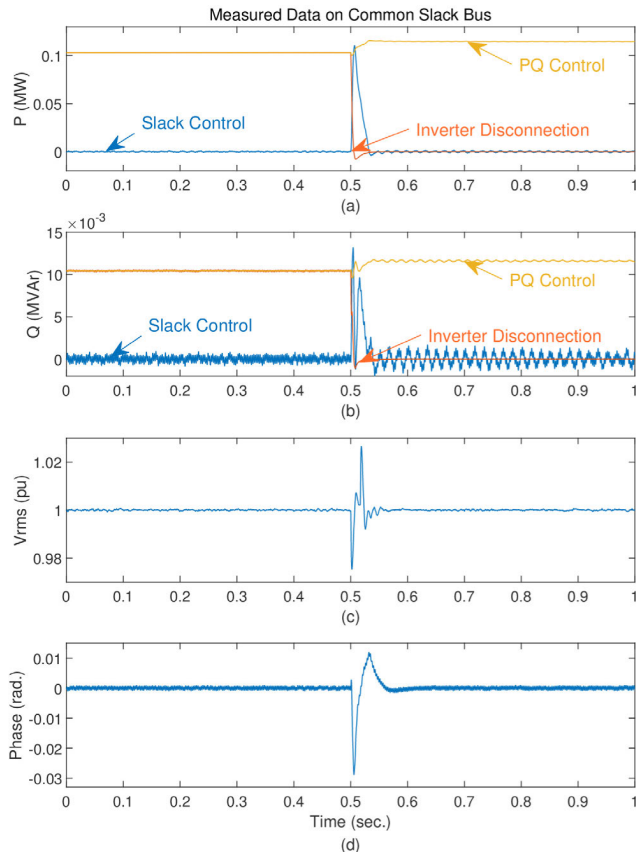

FIGURE 8. Connection of the PQ-control mode inverter at 0.5 seconds: slack control mode inverter (blue line), additionally connected inverter (orange line), and a representative of existing PQ-control mode inverters (yellow line).

power of the newly connected inverter from zeros to 0.1 MW and 0.01 MVAr for one second as shown in Figs. 8(a)-(b). Meanwhile, the DG controller decreases the output powers of the other PQ-control mode inverters from approximately 0.111 MW and 0.0111 MVAr to 0.1 MW and 0.01 MVAr to maintain the average output power of the slack control mode inverter at zero.

C. PQ INVERTER DISCONNECTION
In previous case studies, there have been negligible magnitude and phase angle variations in bus voltages when the slack inverter is disconnected or an additional inverter is connected. This is because the output power time derivatives are very small in both cases at the event. From the viewpoint of the power time derivatives, disconnection of the PQ-control mode inverter might be the most severe event. To evaluate the performance, one of the PQ-control mode inverters is set to be disconnected at 0.5 seconds. As shown in Figs. 9(a)-(b), the slack inverter instantly increases the power to complement the slowly increasing power of the PQ-control mode inverters. The instant power changes of the slack-control mode inverter cause magnitude and phase angle differences of the voltages between the common slack

FIGURE 9. Disconnection of the PQ-control mode inverter at 0.5 seconds: slack control mode inverter (blue line), disconnected inverter (orange line), and a representative of existing PQ-control mode inverters (yellow line).

FIGURE 10. Responses to disconnection of the DG in bus 23 at 0.5 seconds: the main generator in bus 1 (left) and the DG in bus 9 (right).
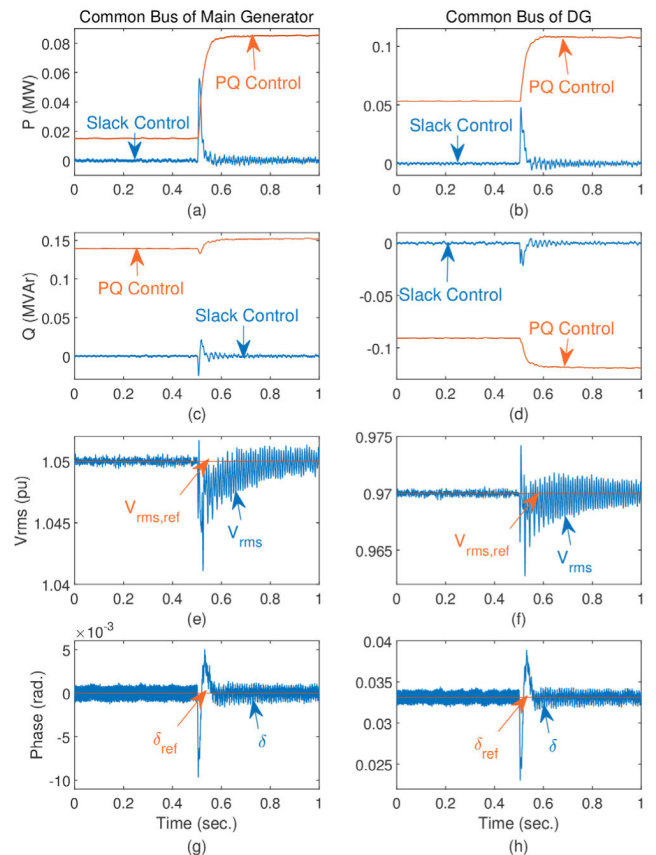
bus and terminal bus of the slack-control mode inverter. These differences are reflected in the common slack bus, as shown in Figs. 9(c)-(d). Although the magnitude and phase angle variations in the voltages become larger than 0.02 pu and 0.03 rad, respectively, they restore their normal values within 0.1 seconds.

VI. CASE STUDIES WITH EXTERNAL CHANGES
The base case output powers of the generators in buses 1, 9, and 23 are approximately 0.75MW/0.06MVAr, 0.4MW/0.03 MVAr, and 0.7 MW/0.13MVAr, respectively.

A. DG DISCONNECTION
Disconnection of a DG is one of the most severe events in the stand-alone microgrid. The performance of the proposed scaled-up slack DG is evaluated by inspecting the main generator and the DG in bus 9 at 0.5 seconds at which the DG in bus 23 is disconnected. The PQ-control mode inverters share the steady-state load based on equations (3) and (4) by themselves in both the main generator and the DG, as shown in Figs. 10(a)-(d). Therefore, the slack-control mode inverters maintain their output powers close to zero at the steady state. Meanwhile, the slack-control mode inverters supply meaningful powers at the moment of the DG disconnection to

complement the time-delayed response of the PQ-control mode inverters. Although the DG in bus 23 is in charge of more than one-third of the entire load consumption, the scaled-up slack makes the disconnection of the DG not severely impact the magnitudes and phase angles of the voltages, as shown in Figs. 10(e)-(h).

B. VOLTAGE REFERENCES CHANGE
According to [5], the magnitude and phase angle of the DG voltage must be controlled very accurately to supply proper real and reactive powers. Therefore, it is very important how accurate and fast the DG controls its magnitude and phase angle. To verify the control performance, the voltage and phase angle references of two DGs are changed while those of the main generator are fixed. As shown in Figs. 11(g)-(i), all generators successfully control their output voltages after a short moment of transients. In the same manner, the phase angles track the references successfully, as shown in Figs. 11(j)-(l). The power injections of the generators are determined by the conditions of the microgrid. As shown in Figs. 11(a)-(f), the real and reactive powers of the slack-controlled inverters are almost maintained at zero, except for small transients. This is because the PQ-control mode inverters properly respond to changes in the microgrid operation.
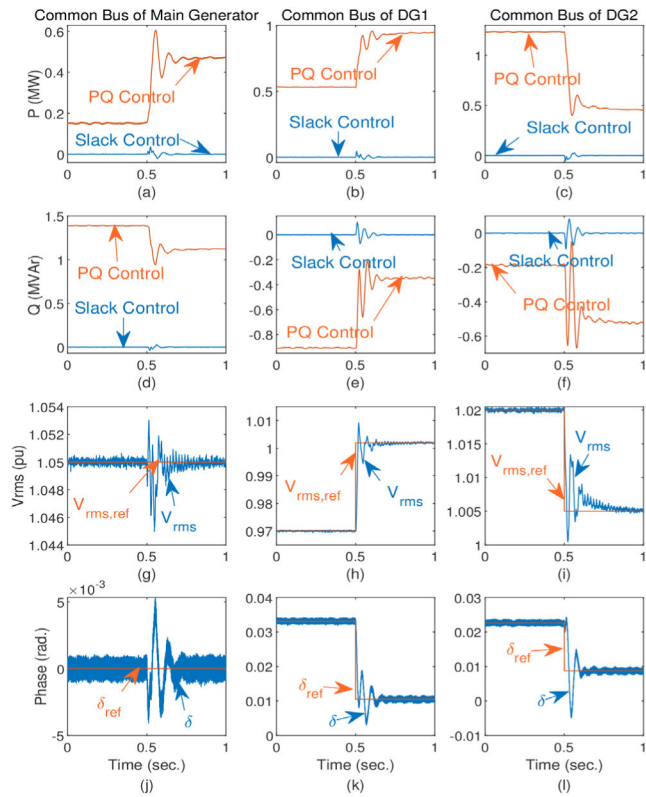
FIGURE 11. Responses of the main generator (left), DG1 (center), and DG2 (right) to voltage reference changes.

FIGURE 12. Responses of the main generator (left), DG1 (center), and DG2 (right) to a load change.

C. LOAD CHANGE

To verify the performance of the proposed scaled-up slack generator in response to load change, a total load of 1.87 MW/ 0.26 MVAr load is reduced to 0.71 MW/0.12 MVAr. The proposed scaled-up slack generators properly respond to the load change. As shown in Figs. 12(a)-(f), the slack-control mode inverters complement the instant power mismatches among the changed load and the power from PQ-control mode inverters. As a result, the magnitudes and phase angles of the voltages are maintained constant after a short transient, as shown in Figs. 12(g)-(l).

VII. CASE STUDIES WITHOUT UPPER-LEVEL CONTROL

One of the most important functions of the IFSA microgrid is the operation without the signal from the upper-level operation system [5]. All of the DGs control their magnitudes and phase angles of voltages using preset references when the upper-level control is lost; in this study, the preset references are selected as 1 pu and 0 radian, respectively. The case studies VI-A and VI-C are conducted again without the upper-level operation signals.

A. DG DISCONNECTION

The performance of the proposed scaled-up slack DG is evaluated by inspecting the main generator and the DG in bus 9 at 0.5 seconds at which the DG in bus 23 is disconnected.
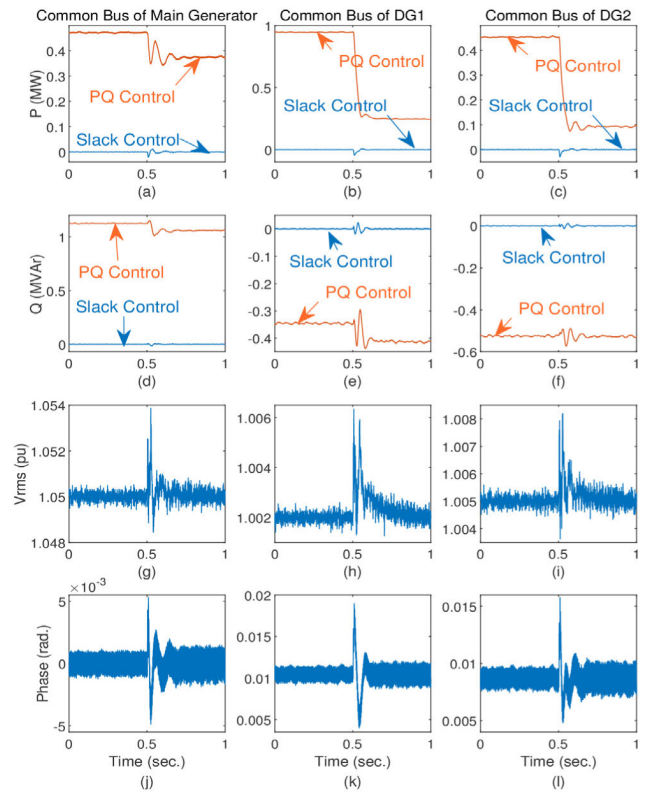
The PQ-control mode inverters share the steady-state load based on equations (3) and (4) by themselves in both the main generator and the DG, as shown in Figs. 13(a)-(d). Therefore, the slack-control mode inverters maintain their output powers close to zero at the steady state. Meanwhile, the slack-control mode inverters supply meaningful powers at the moment of the DG disconnection to complement the time-delayed response of the PQ-control mode inverters. Although the DG in bus 23 is in charge of more than one-third of the entire load consumption, the scaled-up slack makes the disconnection of the DG not severely impact the magnitudes and phase angles of the voltages, as shown in Figs. 13(e)-(h). The magnitudes and phase angles of the voltages are maintained at 1 pu and 0 radians.

B. LOAD CHANGE

The total load of 1.87 MW/0.26 MVAr load is reduced to 0.71 MW/0.12 MVAr. The proposed scaled-up slack generators properly respond to the load change. As shown in Figs. 14(a)-(f), the slack-control mode inverters complement the instant power mismatches among the changed load and the power from PQ-control mode inverters. As a result, the magnitudes and phase angles of the voltages are maintained at 1 pu and 0 radians, respectively, after a short transient, as shown in Figs. 14(g)-(l).
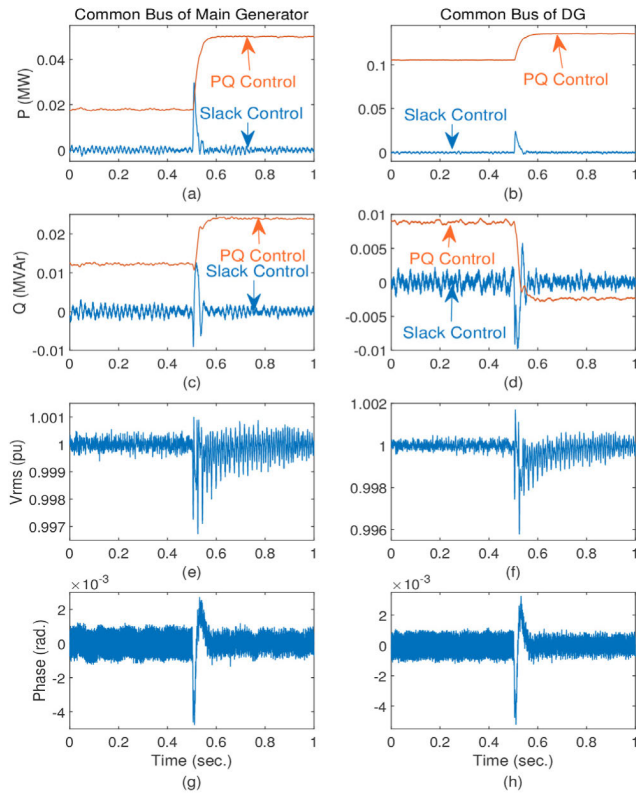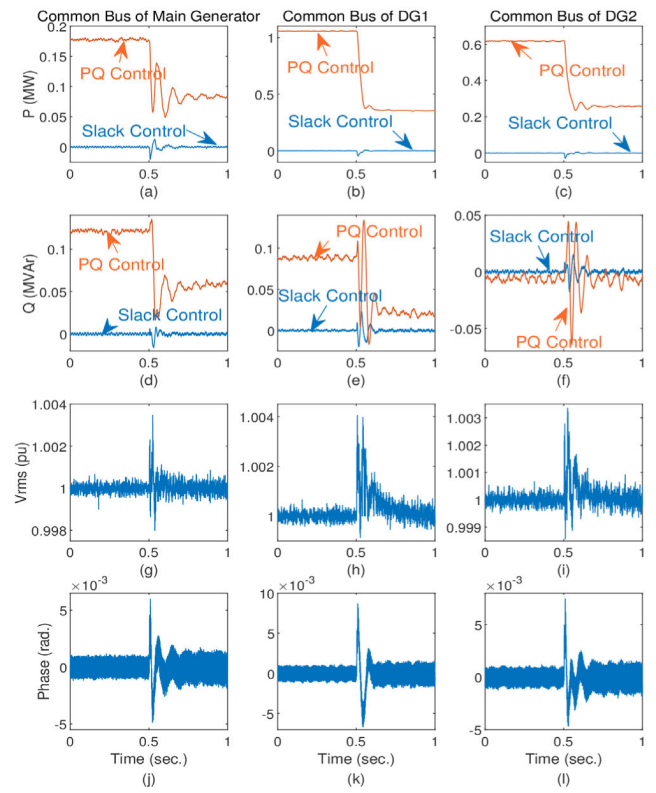
FIGURE 13. Responses to disconnection of the DG in bus 23 at 0.5 seconds: the main generator in bus 1 (left) and the DG in bus 9 (right) without upper-level control.

FIGURE 14. Responses of the main generator (left), DG1 (center), and DG2 (right) to a load change without upper-level control.
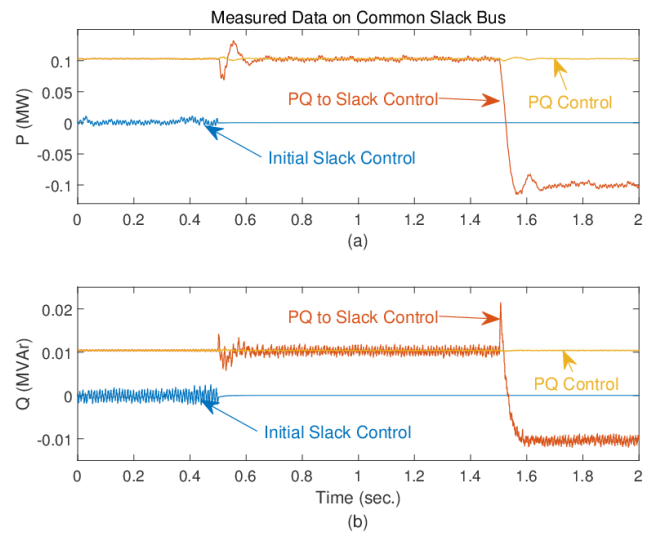
VIII. COMPARISON WITH OTHER METHODS

Many of the previously introduced method in Section I-*B* are not suitable for instant load sharing between inverters in a single bus. This is because they require huge computational effort for load sharing without time delay. In considerations of the computational effort, only droop-based load sharing is sufficiently light for the instant response in the previously addressed methods. By the way, what the droop control has in common is that it needs to measure voltage and frequency (i.e. phase).

A. FIXED SLACK AND DROOP-BASED PQ CONTROL

In general, the slack-controlled inverter is controlled by (5) to ensure robustness of the grid despite the improved stability of [11]. Therefore, the average frequency is maintained in constant even if the PQ-controlled inverters shake the common slack bus. To inspect the fixed slack effect to the droop control, 1 MW/60 Hz and 0.01 MVAr/1 Vpu droop ratios are applied to the PQ-controlled inverters. Fig. 15 shows the result of applying P-f and Q-V droop to the PQ-controlled inverter in the Section V-A. The PQ-controlled inverter must reduce its output to zero to reserve power when its control mode is changed to slack as shown in Fig. 7. However, the droop-based PQ-controlled inverter does not properly operate between 0.5 and 1.5 seconds as shown in Fig. 15. Also, the slack-controlled inverter absorbs rather than

FIGURE 15. Inverter responses to the initial slack control mode inverter disconnection (0.5 seconds) and 20% load disconnection (1.5 seconds): slack inverters with fixed frequencies (blue & orange lines) and droop-based PQ-control mode inverters (yellow line).

supplies power when 20% of the load is disconnected at 1.5 seconds. In other words, the droop-based PQ-controlled inverters do not properly reduce their output powers due to no grid frequency deviation.
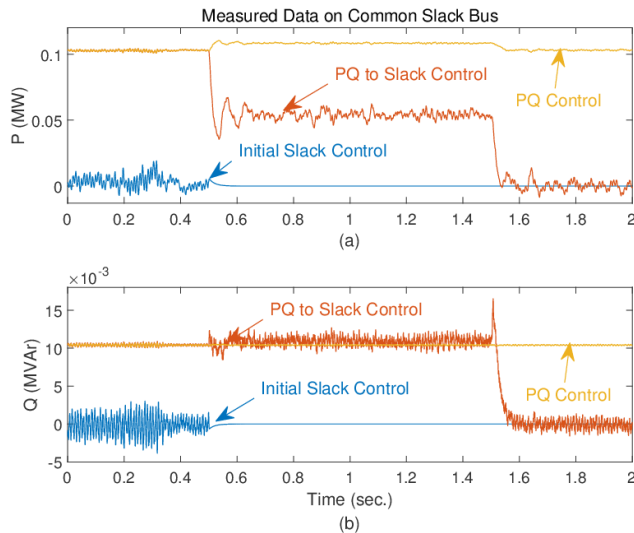
FIGURE 16. Inverter responses to the initial slack control mode inverter disconnection (0.5 seconds) and 10% load disconnection (1.5 seconds): slack inverters with droop based variable frequencies (blue & orange lines) and droop-based PQ-control mode inverters (yellow line).

B. DROOP BASED SLACK & PQ CONTROL

Both the frequency and power of the synchronous generator are controlled by the governor, so they are mutually dependent. Therefore, the inverter, designed to emulate the synchronous generator, can have dependency between the frequency and power [18]–[21]. It means that even slack role inverter has variable frequency rather than a fixed one for power control. By the way, in the IFSA microgrid, the frequency can be only estimated by the electrical measurement due to the absence of the physical rotor. And thus, the measured frequency might have much noise caused by harmonics. Therefore, a high droop ratio might cause system instability from the power oscillation responding to the noise. To inspect the effectiveness of the droop control, a 10 MW/60 Hz droop ration is applied to the slack-inverter. Also, 1 MW/60 Hz and 0.01 MVAr/1 Vpu droop ratios are applied to the PQ-controlled inverters. Fig. 16 shows the result of applying variable frequency inverter to Section VIII-A instead of the fixed slack inverter. The real power of the PQ-controlled inverters increases by the droop control, so the power of the slack-controlled inverter is decreased as shown in Fig. 16(a). Meanwhile, the real power ripple of the slack between 0.5 and 1.5 seconds is larger than that in Fig. 15(a) due to the droop ratio of slack. Related to this, the system cannot operate stably when a larger droop ratio is used. That is, the droop ratio cannot be increased to make the output power of slack be zero. In addition, 10% is the marginal possible load decrease for the stable operation as shown after 1.5 seconds in Fig. 16(a). Related to this, the system cannot operate stably when more than 10% of the load is disconnected.

IX. CONCLUSION

This paper proposed a scaled-up slack generator based on parallel inverters for reliable IFSA microgrids. The proposed

method increased the size of the inverter-based distributed generation (DG), without requiring a size upgrade of each inverter by simply increasing the number of inverters.

To verify the performance of the proposed method, parallel inverters were applied to the DG models in the practical power system model and simulated by the electromagnetic transient program (EMTP). The proposed scaled-up slack generators successfully played a key role in the IFSA microgrid by maintaining constant connected bus voltages. As a result, a large renewable energy could support the grid voltage even if its size is greater than that of the largest individual inverter.

In this study, the performance was verified within the ranges of practical system parameters. However, it is expected that further studies are required to apply the proposed method to a system with an extremely large range of parameters.

It would be expected that the proposed method encourages the expansion of renewable energies by enabling the DGs to support the power system voltage instead of disrupting it.

REFERENCES

[1] V. M. Delmotte, P. Zhai, H. O. Pörtner, D. Roberts, J. Skea, P. R. Shukla, A. Pirani, W. M. Okia, C. Péan, R. Pidcock, S. Connors, J. B. R. Matthews, Y. Chen, X, Zhou, M. I. Gomis, E. Lonnoy, T. Maycock, M. Tignor, and T. Waterfield, "Global warming of 1.5 °C," IPCC Special Rep., Oct. 2018.

[2] *Renewable Energy 3020*, Ministry Trade, Ind. Energy, Sejong City, South Korea, Feb. 2017.

[3] L. G. Meegahapola, S. Bu, D. P. Wadduwage, C. Y. Chung, and X. Yu, "Review on oscillatory stability in power grids with renewable energy sources: Monitoring, analysis, and control using synchrophasor technology," *IEEE Trans. Ind. Electron.*, vol. 68, no. 1, pp. 519–531, Jan. 2021.

[4] S. Maihemuti, W. Wang, H. Wang, J. Wu, and X. Zhang, "Dynamic security and stability region under different renewable energy permeability in IENGS system," *IEEE Access*, vol. 9, pp. 19800–19817, Jan. 2021.

[5] S. H. Lee, D. Choi, and J.-W. Park, "Inertia-free stand-alone microgrid— Part I: Analysis on synchronized GPS time-based control and operation," *IEEE Trans. Ind. Appl.*, vol. 54, no. 5, pp. 4048–4059, Sep./Oct. 2018.

[6] Y. Gui, Q. Xu, F. Blaabjerg, and H. Gong, "Sliding mode control with grid voltage modulated DPC for voltage source inverters under distorted grid voltage," *CPSS Trans. Power Electron. Appl.*, vol. 4, no. 3, pp. 244–254, Sep. 2019.

[7] Y. Zhang, Z. Wang, J. Jiao, and J. Liu, "Grid-voltage sensorless model predictive control of three-phase PWM rectifier under unbalanced and distorted grid voltages," *IEEE Trans. Power Electron.*, vol. 35, no. 8, pp. 8663–8672, Aug. 2020.

[8] W. Deng, N. Dai, K.-W. Lao, and J. M. Guerrero, "A virtual-impedance droop control for accurate active power control and reactive power sharing using capacitive-coupling inverters," *IEEE Trans. Ind. Appl.*, vol. 56, no. 6, pp. 6722–6733, Nov./Dec. 2020.

[9] M. M. Bijaieh, W. W. Weaver, and R. D. Robinett, "Energy storage requirements for inverter-based microgrids under droop control in d-q coordinates," *IEEE Trans. Energy Convers.*, vol. 35, no. 2, pp. 611–620, Jun. 2020.

[10] A. G. Paspatis, G. C. Konstantopoulos, and J. M. Guerrero, "Enhanced current-limiting droop controller for grid-connected inverters to guarantee stability and maximize power injection under grid faults," *IEEE Trans. Control Syst. Technol.*, vol. 29, no. 2, pp. 841–849, Mar. 2021.

[11] G. Raman and J. C.-H. Peng, "Mitigating stability issues due to line dynamics in droop-controlled multi-inverter systems," *IEEE Trans. Power Syst.*, vol. 35, no. 3, pp. 2082–2092, May 2020.

[12] E. Lenz, D. J. Pagano, A. Ruseler, and M. L. Heldwein, "Two-parameter stability analysis of resistive droop control applied to parallel-connected voltage-source inverters," *IEEE J. Emerg. Sel. Topics Power Electron.*, vol. 8, no. 4, pp. 3318–3332, Dec. 2020.

[13] G. Raman, J. C.-H. Peng, and H. H. Zeineldin, "Optimal damping recovery scheme for droop-controlled inverter-based microgrids," *IEEE Trans. Smart Grid*, vol. 11, no. 4, pp. 2805–2815, Jul. 2020.

[14] S. M. Mohiuddin and J. Qi, "Droop-free distributed control for AC micro-grids with precisely regulated voltage variance and admissible voltage pro-file guarantees," *IEEE Trans. Smart Grid*, vol. 11, no. 3, pp. 1956–1967, May 2020.

[15] J. Lai, X. Lu, X. Yu, and A. Monti, "Stochastic distributed secondary control for AC microgrids via event-triggered communication," *IEEE Trans. Smart Grid*, vol. 11, no. 4, pp. 2746–2759, Jul. 2020.

[16] C. Roncero-Clemente, E. Gonzalez-Romera, F. Barrero-Gonzalez, M. I. Milanes-Montero, and E. Romero-Cadaval, "Power-flow-based secondary control for autonomous droop-controlled AC nanogrids with peer-to-peer energy trading," *IEEE Access*, vol. 9, pp. 22339–22350, Feb. 2021.

[17] N. Nasser and M. Fazeli, "Buffered-microgrid structure for future power networks; a seamless microgrid control," *IEEE Trans. Smart Grid*, vol. 12, no. 1, pp. 131–140, Jan. 2021.

[18] O. Babayomi and S. University, "Distributed secondary frequency and voltage control of parallel-connected VSCs in microgrids: A predictive VSG-based solution," *CPSS Trans. Power Electron. Appl.*, vol. 5, no. 4, pp. 342–351, Dec. 2020.

[19] X. Meng, J. Liu, and Z. Liu, "A generalized droop control for grid-supporting inverter based on comparison between traditional droop control and virtual synchronous generator control," *IEEE Trans. Power Electron.*, vol. 34, no. 6, pp. 5416–5438, Jun. 2019.

[20] M. Mao, C. Qian, and Y. Ding, "Decentralized coordination power control for islanding microgrid based on PV/BES-VSG," *CPSS Trans. Power Electron. Appl.*, vol. 3, no. 1, pp. 14–24, Mar. 2018.

[21] W. Wang, L. Jiang, Y. Cao, and Y. Li, "A parameter alternating VSG controller of VSC-MTDC systems for low frequency oscillation damping," *IEEE Trans. Power Syst.*, vol. 35, no. 6, pp. 4609–4621, Nov. 2020.

[22] G. A. Ramos, R. I. Ruget, and R. Costa-Castello, "Robust repetitive control of power inverters for standalone operation in DG systems," *IEEE Trans. Energy Convers.*, vol. 35, no. 1, pp. 237–247, Mar. 2020.

[23] X. Wang, Y. Lin, B. Wang, W. Liu, and K. Bai, "Output voltage control of BESS inverter in stand-alone micro-grid based on expanded inverse model," *IEEE Access*, vol. 8, pp. 3781–3791, Jan. 2020.

[24] D. Choi, J.-W. Park, and S. H. Lee, "Virtual multi-slack droop control of stand-alone microgrid with high renewable penetration based on power sensitivity analysis," *IEEE Trans. Power Syst.*, vol. 33, no. 3, pp. 3408–3417, May 2018.

[25] D. Kim, J. W. Park, and S. H. Lee, "A study on the power reserve of distributed generators based on power sensitivity analysis in a large-scale power system," *Electronics*, vol. 10, no. 7, pp. 1–13, Mar. 2021.

[26] J. Saha, D. Hazarika, N. B. Y. Gorla, and S. K. Panda, "Machine learning aided optimization framework for design of medium-voltage grid-connected solid-state-transformers," *IEEE J. Emerg. Sel. Topics Power Electron.*, early access, Apr. 20, 2021, doi: 10.1109/JESTPE.2021.3074408.

[27] J. Saha, G. N. B. Yadav, and S. K. Panda, "A review on bidirectional matrix-based AC-DC conversion for modular solid-state-transformers," in *Proc. IEEE 4th Int. Future Energy Electron. Conf. (IFEEC)*, Nov. 2019, pp. 1–8.

SOO HYOUNG LEE (Member, IEEE) received the B.S. and Ph.D. degrees in electrical engineering from the School of Electrical and Electronic Engineering, Yonsei University, Seoul, South Korea, in 2008 and 2012, respectively. From 2012 to 2014, he was a Postdoctoral Research Associate with the School of Electrical and Computer Engineering, Georgia Institute of Technology, Atlanta, GA, USA. From 2014 to 2018, he was a Senior Researcher with the Advanced Power Grid Research Division, Korea Electrotechnology Research Institute, Uiwang, South Korea. He is currently an Assistant Professor with the Department of Electrical and Control Engineering, Mokpo National University, Mokpo, South Korea. His research interests include converter-based microgrid, optimal coordination of distributed generation systems, converter control for distributed generation systems, implementation of multi-level converters for low voltage ac systems, and non-isolated dc–dc converters for high voltage applications.

• • •